Hindawi Publishing Corporation
EURASIP Journal on Advances in Signal Processing
Volume 2008, Article ID 837102, 12 pages
doi:10.1155/2008/837102

Research Article

Experimental Evaluation of Adaptive Modulation and Coding in MIMO WiMAX with Limited Feedback

Christian Mehlführer, Sebastian Caban, and Markus Rupp

Institute of Communications and Radio-Frequency Engineering, Vienna University of Technology, Gusshausstrasse 25/389, 1040 Vienna, Austria

Correspondence should be addressed to Christian Mehlführer, christian.mehlfuehrer@nt.tuwien.ac.at

Received 22 June 2007; Revised 3 October 2007; Accepted 28 November 2007

Recommended by Ana Pérez-Neira

We evaluate the throughput performance of an OFDM WiMAX (IEEE 802.16-2004, Section 8.3) transmission system with adaptive modulation and coding (AMC) by outdoor measurements. The standard compliant AMC utilizes a 3-bit feedback for SISO and Alamouti coded MIMO transmissions. By applying a 6-bit feedback and spatial multiplexing with individual AMC on the two transmit antennas, the data throughput can be increased significantly for large SNR values. Our measurements show that at small SNR values, a single antenna transmission often outperforms an Alamouti transmission. We found that this effect is caused by the asymmetric behavior of the wireless channel and by poor channel knowledge in the two-transmit-antenna case. Our performance evaluation is based on a measurement campaign employing the Vienna MIMO testbed. The measurement scenarios include typical outdoor-to-indoor NLOS, outdoor-to-outdoor NLOS, as well as outdoor-to-indoor LOS connections. We found that in all these scenarios, the measured throughput is far from its achievable maximum; the loss is mainly caused by a too simple convolutional coding.

1. INTRODUCTION

With the theoretical understanding of the nature of multiple antenna systems in a scattering environment by Winters [1], Foschini and Gans [2], and Telatar [3], an enormous potential for high spectral efficiency was found. This gave the motivation to include multiple antenna systems in wireless transmission standards like UMTS [4], WiMAX [5], and WLAN [6]. A summary of all these standardization efforts is given in [7]. They have in common that the amount of feedback information is limited to a few bits per transmission frame, preventing the implementation of optimal beamforming solutions [8–10] that allow for close-to-capacity performance.

In this work, we measure the throughput performance of a SISO/MIMO OFDM system that uses the coding and modulation schemes defined in the WiMAX standard IEEE 802.16-2004 [5, Section 8.3], and [11]. The feedback mechanism in WiMAX is limited to 3 bits by which one out of seven possible adaptive modulation and coding (AMC) schemes is selected, for example, depending on the received SNR.

Multiple transmit antennas are incorporated into the WiMAX standard by Alamouti space-time coding [12] at the transmitter, thus increasing the available receive SNR and the spatial diversity. This allows to reuse the same feedback as in the SISO case for the Alamouti coded system. In addition to Alamouti space-time coding, we consider spatial multiplexing with individual AMC at every of the two transmit antennas as an extension to the WiMAX standard [13]. In particular, four different transmission modes were implemented and measured.

(Mode 1) This mode is the standardized single transmit antenna system with 3-bit feedback.

(Mode 2) This is the standardized two-transmit-antenna system with Alamouti coding with also 3-bit feedback.

(Mode 3) This is a spatial multiplexing, that is, two-transmit-antenna system using 3-bit feedback

(equal coding rate at both antennas). This mode is incorporated in the following mode but its throughput is evaluated separately.

(Mode 4) This is a spatial multiplexing, two-transmit-antenna system using 6-bit feedback (individual coding rate at both antennas).

The measured data throughput of these transmission modes is compared to the mutual information of the wireless channel when the transmitter has no channel knowledge.

Previous work in this field is based either on simulations [14–16] or on channel sounding experiments that yield channel coefficients and channel capacities for different scenarios [17, 18]. To the authors' knowledge, no work exists so far where the data throughput of a MIMO WiMAX system is measured and compared to the mutual information of the channel. Such a comparison is of utmost importance to identify potential weaknesses of a transmission system and to propose possible enhancements.

The paper is organized as follows. Section 2 presents the transmitter and receiver algorithms used to generate the transmit signals and to evaluate the receive signals, respectively. Section 3 provides an overview of the Vienna MIMO testbed and the setup of transmitter and receiver in our measurement scenarios. In Section 4, we introduce a so-called "perfect" AMC feedback method. Section 5 includes a derivation of the achievable data throughput based on the mutual information of the channel. The measured data throughput is presented in Section 6. In Section 7, we draw our conclusions. In Appendix A we substantiate our findings from the measurement results by simulating the system performance in a well-defined environment. Finally, in Appendix B the SNR gains of improved channel estimators are evaluated.

2. BASEBAND PROCESSING

In this section, the data generation at the transmitter and the data processing at the receiver are explained for the four different transmission modes considered in our experiments. Specifically, we distinguish between SISO/SIMO transmission, MISO/MIMO transmission with Alamouti space-time coding, and MIMO transmission with spatial multiplexing. In the case of a single transmit antenna and for Alamouti mode, a single data stream is transmitted, while for spatial multiplexing, two independently coded and modulated data streams are transmitted.

2.1. Transmitter

At first, random data bits are generated and then coded by a concatenated Reed-Solomon (RS) and convolutional encoder (see Figure 1). The systematic outer RS code uses a codeword length of 255 bytes, a data length of 239 bytes, and a parity length of 16 bytes. Depending on the currently selected AMC value, the RS code is shortened (to allow for smaller block sizes) and punctured. The outer convolutional code of rate $R = 1/2$ is generated by the polynomials 171_{OCT} and 133_{OCT}. This code belongs to the class of the so-called maximum free distance codes with constraint length seven. However, after puncturing depending on the AMC value, the maximum free distance is reduced to $d_{\mathrm{free}} = 6$ for $R = 2/3$, $d_{\mathrm{free}} = 5$ for $R = 3/4$, and $d_{\mathrm{free}} = 4$ for $R = 5/6$, respectively, $d_{\mathrm{free}} = 10$).

After coding, an interleaver is implemented to avoid long runs of low reliable bits at the decoder input. The interleaved bits are mapped adaptively to a symbol alphabet. The coding, interleaving, and symbol mapping are the same as defined in the WiMAX IEEE 802.16-2004 specification [5]. Depending on the feedback information from the receiver, the mapping and the coding rate are adjusted. The seven possibilities for the AMC schemes are summarized in Table 1. When Alamouti transmission is selected, the symbols are additionally space-time coded to generate the transmit symbols for both antennas. For spatial multiplexing, the SISO encoding and modulation mapping are used for both transmit antennas separately, leading to a total number of $7 \times 7 = 49$ AMC schemes.

After mapping the bits to symbols, serial-to-parallel conversion is carried out to form OFDM symbols (256 carrier OFDM with 192 data symbols). Pilots, training symbols, a zero DC carrier, and guard carriers are added as defined in [5]. After an inverse fast Fourier transformation (IFFT), a cyclic prefix is added. We chose a cyclic prefix length of 1/4 of the total OFDM symbol length to avoid intersymbol interference in all measurement scenarios. Before transmitting over the wireless channel, the signal is normalized by a factor $1/\sqrt{N_T}$ (with N_T corresponding to the number of transmit antennas), ensuring equal total signal power for single and multiple antenna transmissions. Note that base stations are subject to a power constraint by the telecommunications regulator. To satisfy such a constraint, we introduced the above normalization. Therefore, in SISO transmissions the single transmit antenna radiates twice the power of each (2 TX) MIMO antenna.

2.2. Receiver

At the receiver, we first perform the inverse operations of the transmitter, that is, cyclic prefix removal, FFT, extraction of data carriers and training symbols. The training symbols (one symbol on the even subcarriers of transmit antenna one and one symbol on the odd subcarriers of transmit antenna two) are used for least-squares channel estimation. The least-squares channel estimator was chosen here since it is of very low complexity. (Note that according to the standard [5] for the WiMAX training sequences, the least squares channel estimation reduces to one multiplication per estimated channel coefficient.) For reference purposes an LMMSE channel estimator and a genie driven channel estimator that uses all data symbols for channel estimation were also implemented. (The noise variance, required for LMMSE channel estimation [19], was estimated at the zero DC carrier. This is possible because we are using a low intermediate frequency avoiding IQ imbalance problems. Note also that transmitter and receiver were synchronized by means of Rubidium frequency standards avoiding frequency offsets between the oscillators.). Unless otherwise stated,

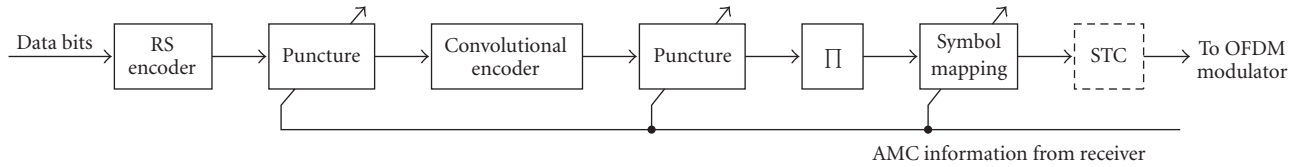

Figure 1: Encoding and modulation at the transmitter.

Table 1: The WiMAX AMC schemes in our setup for single antenna and Alamouti transmission. For spatial multiplexing, a separate AMC scheme can be used for every transmit antenna. These frame sizes correspond to 44 OFDM data symbols transmitted in a frame duration of 2.5 milliseconds.

AMC scheme	Data bits per frame	Modulation	Coding rate	Max. throughput
(1)	4224	2-PAM	1/2	1.69 Mbps
(2)	8448	4-QAM	1/2	3.38 Mbps
(3)	12672	4-QAM	3/4	5.07 Mbps
(4)	16896	16-QAM	1/2	6.76 Mbps
(5)	25344	16-QAM	3/4	10.14 Mbps
(6)	33792	64-QAM	2/3	13.52 Mbps
(7)	38016	64-QAM	3/4	15.21 Mbps

all measurement results are based on least-squares channel estimation.

The channel estimates and the data symbols are passed to a max-log-MAP (maximum a posteriori) demapper. The demapper for the spatial multiplexing transmissions is implemented as a soft output sphere decoder with a single-tree search [20]. The resulting soft bits are passed to a Viterbi decoder and then to a Reed-Solomon decoder.

3. MEASUREMENTS

When it comes to measuring systems with feedback, there are basically three approaches.

(i) One might build a demonstrator [21] where the whole system (including the feedback) [22] is implemented in real-time.

(ii) One might use a testbed where the received data is evaluated "quickly" (e.g., in Matlab or C) and the feedback is carried out via a LAN-connection. In such a scenario, round trip times (receiver algorithm in Matlab + LAN + transmitter algorithm in Matlab + loading the data into the testbed) are usually in the order of 100 milliseconds up to a second, depending on the effort put into the implementation. This feedback method is especially interesting for indoor scenarios where the channel stays constant over such long periods of time, if carried out, for example, at night. In outdoor scenarios, trees, cars, and other constantly moving uninfluenceable objects may prohibit such a measurement.

(iii) One might not use feedback at all but transmit a block of data for every possible feedback combination, to evaluate these blocks later on. Of course, this is only realizable in the case of limited feedback.

Approaches one and two require the knowledge of some method to select the AMC scheme. These two approaches are not applicable if the method of extracting the feedback bits from the received data is yet to be found. Also, only one particular feedback method can be investigated in one measurement. We therefore decided to implement the third approach, explained in detail in the following. This approach has the advantage that also an optimal feedback method can be investigated allowing to benchmark other realistic methods based on, for example, the received SNR.

3.1. Measurement setup

For our measurements, we utilize the Vienna MIMO testbed described in [23] enhanced by new power and low-noise amplifiers. The basic features of the testbed are as follows.

(i) Baseband processing is carried out offline in Matlab with floating-point precision. The transmitted and received down-sampled signals are stored on hard disk drives (approximately 600 Gbytes per scenario measured).

(ii) Receiver and transmitter are synchronized by means of rubidium frequency standards and a LAN connection.

(iii) The carrier frequency is 2.5 GHz; the bandwidth is 5 MHz.

(iv) The two transmit antennas [24] are mounted on a pole 16 meters above rooftop (downtilt ten degrees) with a horizontal spacing of 2.75λ (see Figure 2). Both antennas have two connectors for +45 and −45 polarized antenna elements. The results presented in this paper are based on measurements which utilized only the +45 polarized elements of each antenna (= two equally polarized antennas, horizontally spaced

by 2.75λ). Reference measurements using the two different polarizations of only one antenna yielded the same conclusions and are therefore not further discussed in this paper.

(v) The receive antennas are placed on a stepper-motor-controlled linear XY positioning table. This table was placed at three positions resulting in the following three measurement scenarios.

(a) In *Scenario 1*, the table was placed two floors below the transmit antenna in the same building having a non-line-of-sight connection.

(b) In *Scenario 2*, the table was placed in a non-line-of-sight connection in the courtyard next to the transmit antenna.

(c) A line-of-sight connection was established in *Scenario 3* by placing the table with the receive antennas in the adjacent building (Figure 2).

These three practical scenarios represent three different locations of a user accessing the internet via a WiMAX connection.

3.2. Measuring a scenario

For each of the scenarios, we transmitted the following blocks of data (Figure 3).

(a) A 2.5-millisecond long block, encoded according to every possible feedback value (AMC value), was transmitted.

(b) Consecutively, 7 SISO blocks, 7 Alamouti coded blocks, and 7×7 blocks employing spatial multiplexing were transmitted.

(c) The resulting $7+7+7\times7 = 63$ blocks were transmitted at 15 different transmit power levels (28 dBm down to -2 dBm in steps of 2 dB) which was achieved by analog attenuation of the transmitted signal prior to the power amplifier.

(d) After reception, the resulting $15\times(7+7+7\times7)$ blocks were stored on hard disks for offline processing in Matlab. The mean performance of a specific scenario was obtained by repeating the above described transmission at 502 different positions of the receive antenna uniformly distributed within an area of $4\lambda \times 4\lambda$ (corresponding to a distance of 0.18λ between the measurement positions). Note that more positions within the same area would not significantly increase the accuracy of the results because the channel realizations become correlated. The only method to increase the number of realizations is to increase the measurement area, but this would lead to undesired large-scale fading effects.

3.3. Measured channels

The method of successively transmitting all AMC schemes requires that the channel stays constant during the transmission of the 63 blocks to obtain meaningful throughput results. Large channel coherence time was achieved by performing the outdoor-to-indoor measurements in the late evening and by locking up the room with the receiver. The outdoor-to-outdoor measurements were also performed in a closed courtyard where no persons/objects moved around.

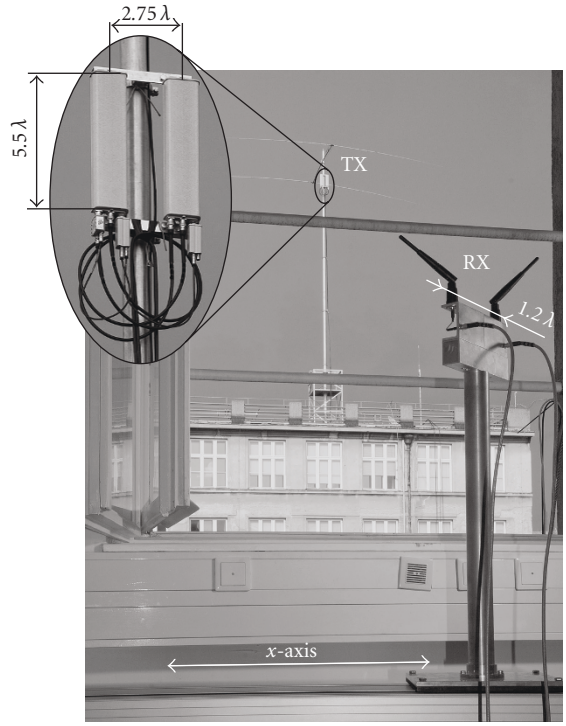

Figure 2: Transmit and receive antenna setups in the outdoor-to-indoor LOS scenario.

The time-invariance of the frequency response from transmit antenna one to receive antenna one is illustrated in Figure 4. In this figure, the *estimated* channel coefficients of the successively transmitted data blocks (at the same overall transmit power level) are plotted on top of each other. The estimated channel coefficients include all amplification and attenuation factors (including transmit power normalization) applied to the signal after the training signal generation. These attenuation factors are thus part of the estimated channel. Because of the transmit power normalization, the frequency responses of the seven SISO AMC schemes are 3 dB larger than the frequency responses of the MIMO AMC schemes. It should be emphasized that the channel characteristics (gain and receiver noise variance) stay constant also for the transmission at different transmit power levels.

Besides the 3 dB normalization factor, all frequency responses in Figure 4 show a very good agreement. The differences between the frequency responses are only given by the channel estimation error. By estimating the same channel with different noise realizations several times in a Matlab simulation, we could verify that the measured errors in the frequency response are in the same order as the channel estimation error.

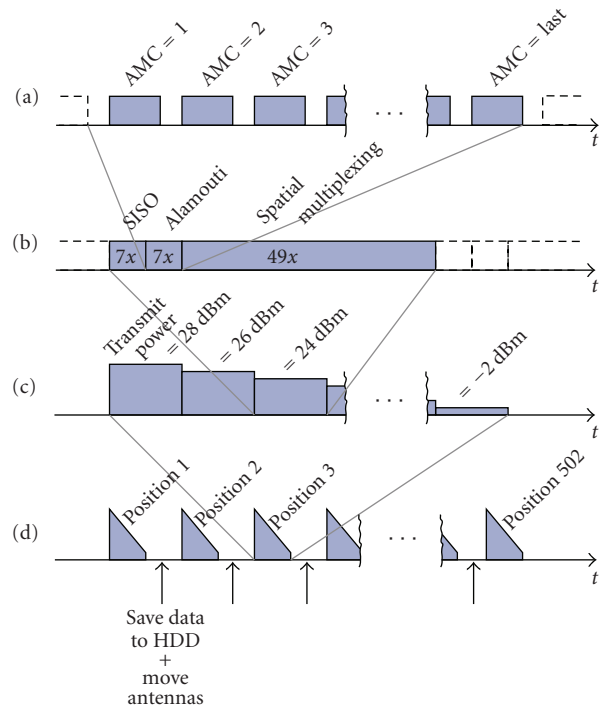

Figure 3: Structure of the transmitted data blocks, (a) is a zoomed version of (b).

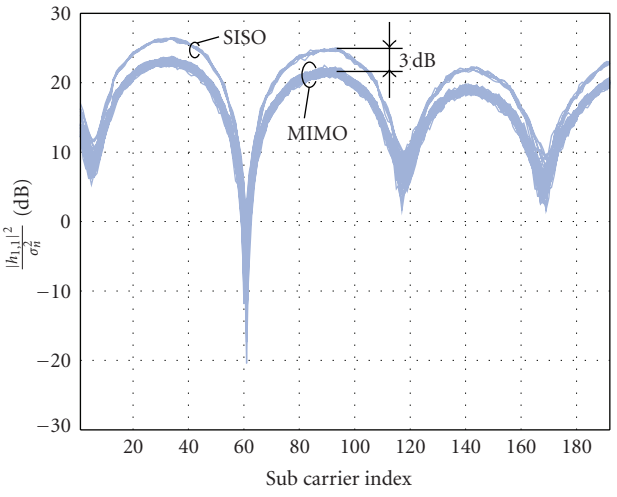

Figure 4: Estimated channel coefficients for the SISO as well as the MIMO cases between transmit antenna one and receive antenna one, scenario 1, NLOS outdoor-to-indoor. The coefficients are plotted over the 192 data subcarriers; the eight pilots and the zero DC carrier are left out. Note that the transmitter attenuation is included in these estimated channel coefficients leading to 3 dB smaller channel coefficients for MIMO transmissions.

Because of the above described reasons, we can consider the scenarios as quasistatic during all transmissions at a given receive antenna position.

4. BEST AMC SELECTION

We define the best possible AMC selection as the one that maximizes the data throughput. Since all AMC schemes are transmitted consecutively over approximately the same channel, we can evaluate all schemes and select the one that achieves the highest throughput. This perfect feedback scheme and the method of calculating the data throughput for this scheme will be explained in the following.

We calculate the data throughput for the following receiver schemes.

Single receive antenna schemes

(i) *SISO transmission of a single data stream*. The receiver selects one of the seven AMC schemes shown in Table 1. This requires a 3-bit feedback for every frame.

(ii) 2×1 *MISO transmission of a single Alamouti space-time coded data stream*. The same AMC schemes as for the SISO transmission are employed.

Dual receive antenna schemes

(i) *SIMO transmission of a single data stream with maximum ratio combining at the receiver*. The same AMC schemes as for the SISO transmission are employed.

(ii) *MIMO transmission of a single Alamouti space-time coded data stream with maximum ratio combining at the receiver*. Again, the same AMC schemes as for the SISO transmission are employed.

(iii) 2×2 *MIMO transmission of two data streams*. Both data streams are encoded by the *same* modulation and coding scheme. The feedback effort here is therefore the same as in the SIMO transmission, that is, 3 bits.

(iv) 2×2 *MIMO transmission of two independent data streams*. Every data stream is encoded and modulated as defined for the SISO transmission, leading to a total combination of $7 \times 7 = 49$ schemes with an overall feedback effort of 6 bits. Note that this mode includes all possible modulation and coding schemes of the previous transmission mode.

At a specific channel realization $c = 1, \ldots, N_{\mathrm{RXpos}}$ and a specific transmit attenuator value $m = 1, \ldots, 15$, we calculate the best instantaneous data throughput as

$$D_{\mathrm{best}}^{(c,m)} = \max_{i \in \mathbb{I}} R_i \left(1 - P_i^{(c,m)}\right), \tag{1}$$

where R_i corresponds to the data rate of the ith adaptive modulation and coding scheme ($i \in \mathbb{I}$, where $\mathbb{I}$ is the set of all adaptive schemes) and $P_i^{(c,m)} \in \{0, 1\}$ is a frame error indicator. (It is convenient here to use a frame error indicator instead of the BER as a basis for the data throughput calculation since at low SNR the BER converges to 0.5. Therefore, simply counting the correctly detected bits would give too large values for the data throughput.) In this work, we assume that one frame is equal to one transmission block defined in Section 3. The data throughput at one transmit attenuation value is found by averaging over all

channel realizations (N_{RXpos} receiver positions) at a specific attenuation m:

$$D_{\mathrm{best,avg}}^{(m)} = \frac{1}{N_{\mathrm{RXpos}}} \sum_{c=1}^{N_{\mathrm{RXpos}}} D_{\mathrm{best}}^{(c,m)}. \quad (2)$$

Note that (2) gives the absolute maximum data throughput that is possible with the available transmission schemes. This data rate can only be achieved by a genie-driven AMC selection that knows the block errors of all transmission schemes already before the actual transmission. In a real system, the selection of an appropriate AMC value would have to rely on the channel state information and the estimated noise variance to predict the block errors for all AMC schemes. The nontrivial problem of selecting the appropriate AMC value is not addressed in this work.

5. ACHIEVABLE DATA THROUGHPUT

In this section, we derive an expression for the "achievable" data throughput that can be used as a performance bound for the measured data throughput. This expression is based on the mutual information between transmit and receive signals, that is, the estimated frequency response. The achievable data throughput is only a function of the wireless channel and does not depend on the AMC schemes used in the measurements.

Consider the mutual information of an AWGN channel with the SNR ρ:

$$I = \log_2\{1 + \rho\}, \quad (3)$$

In theory, a transmission can achieve a rate corresponding to this mutual information. This requires that the transmitter adapts the coding rate to the receive SNR. Therefore, the receiver has to feed back which AMC value the transmitter has to use. In WiMAX, seven AMC schemes corresponding to 3-bit feedback are defined.

The mutual information for transmitting symbols over a MIMO channel (which correspond to the mutual information of the kth subcarrier of the OFDM system) can be expressed as [2, 3]

$$I_k^{(c,m)} = \log_2\left\{ \det\left(\mathbf{I}_{N_R} + \frac{1}{\sigma_n^2} \mathbf{H}_k^{(c,m)} \mathbf{H}_k^{(c,m)H} \right) \right\}. \quad (4)$$

(In literature, the mutual information is often referred to as "capacity without channel knowledge at the transmitter." However, the capacity is a property of the channel and cannot depend on the particular implementation of a transmission system (e.g., with or without full channel knowledge at the transmitter). We will therefore base the calculation of the achievable data throughput on the mutual information.) Equation (4) assumes that the transmitter has no knowledge about the channel, and thus the transmit power is distributed equally over the antennas. Using (4), we can estimate the theoretically achievable transmission rate by substituting the true channel matrix $\mathbf{H}^{(c,m)}$ with the estimated channel matrix $\mathbf{H}_{\mathrm{est}}^{(c,m)}$. To improve the accuracy of the mutual information, we use the channel matrices estimated by the genie-driven channel estimator that utilizes all transmitted data symbols. Additionally, we calculate the channel matrices for large transmit attenuator values from the estimated channel matrix at the smallest transmit attenuator value

$$\mathbf{H}_{\mathrm{est}}^{(c,m)} = \frac{A_m}{A_1} \mathbf{H}_{\mathrm{est}}^{(c,1)}, \quad m = 2, \ldots, 15. \quad (5)$$

Here, A_m denotes the mth transmit attenuation value and A_1 corresponds to the smallest attenuation. The noise variance σ_n^2 is also substituted by the estimated noise variance. It is approximately the same at both receive antennas with a difference of about 1 dB.

The overall mutual information $I_{\mathrm{sum}}^{(m)}$ for the OFDM system at one transmit attenuation value m can now be calculated by summing the mutual information of all subcarriers and averaging over the N_{RXpos} (the realizations) different receiver positions:

$$I_{\mathrm{sum}}^{(m)} = \frac{1}{N_{\mathrm{RXpos}}} \sum_{c=1}^{N_{\mathrm{RXpos}}} \sum_{k=1}^{192} I_k^{(c,m)}. \quad (6)$$

Since the transmission of an OFDM signal requires also the transmission of a cyclic prefix to avoid intersymbol interference, and a preamble for synchronization and channel estimation, the mutual information given by (6) can never be achieved. It is therefore convenient to introduce an "achievable" data throughput $D_{\mathrm{achievable}}^{(m)}$ that accounts for these inherent system losses. We define the achievable data throughput at the transmit attenuation value m as

$$D_{\mathrm{achievable}}^{(m)} = \frac{1}{1+G} \cdot \frac{1/T_s}{256} \cdot \frac{N_{\mathrm{data}}}{N_{\mathrm{OFDM}}} \cdot I_{\mathrm{sum}}^{(m)}, \quad (7)$$

where G (1/4 in our measurements) corresponds to the ratio of cyclic prefix time and useful OFDM symbol time, N_{data} (44 in our measurements) is the number of OFDM data symbols, N_{OFDM} (47 in our measurements) is the total number of OFDM symbols in one transmission frame, and T_s corresponds to the sampling rate of the transmit signal. The factor $(1/T_s)/256$ is therefore equivalent to the available bandwidth per subcarrier. In our measurements, we chose a channel bandwidth of 5 MHz. For this channel bandwidth, the WiMAX standard defines a sampling rate of $T_s = 1/5.76$ MHz. The 5.76 MHz total signal bandwidth emerging from this sampling rate fits into the 5 MHz channel bandwidth because some of the guard band carriers (with zero energy) are outside the 5 MHz channel bandwidth.

Equation (7) will be used as a performance bound for comparisons with the measured data throughput in the next section.

6. RESULTS

In this section, we present the measured data throughput results and give explanations for the observed performance. In order to account for all possible losses in the transmission chain, the curves presented in this section are plotted over the transmit power rather than over the received SNR [25].

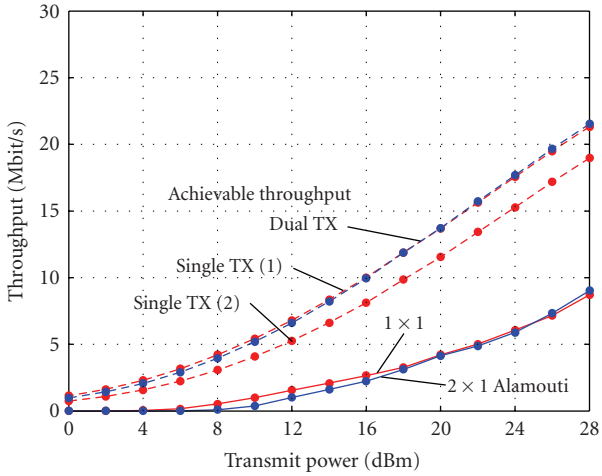

FIGURE 5: Scenario 1, measured (solid) and achievable (dashed) data throughput in the NLOS outdoor-to-indoor scenario using one receive antenna. The largest transmit power corresponds to a receive SNR of about 22 dB.

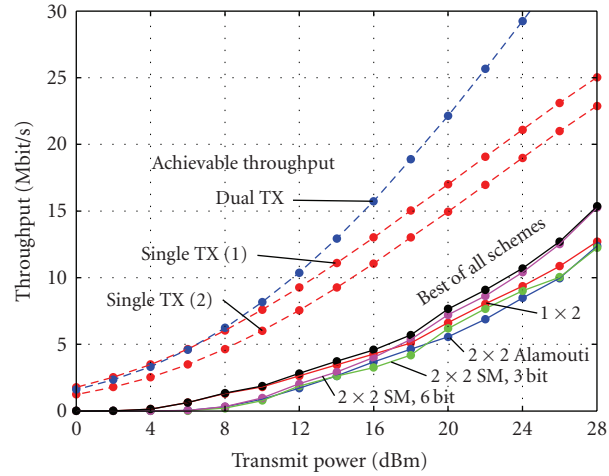

FIGURE 6: Scenario 1, measured (solid) and achievable (dashed) data throughput in the NLOS outdoor-to-indoor scenario using two receive antennas. The largest transmit power corresponds to a receive SNR of about 22 dB.

6.1. *Scenario 1—NLOS outdoor-to-indoor*

In this scenario, the receiver was placed three floors below the transmit antenna mounted on a pole on the roof, resulting in a non-line-of-sight outdoor-to-indoor connection. The scenario is characterized by strong frequency selectivity and hence large frequency diversity. The measured data throughput is shown for one and two receive antennas in Figures 5 and 6, respectively. In Figure 5, we observe that the achievable data throughput is approximately the same for a two-transmit-antenna transmission and a transmission on the first transmit antenna only. The achievable data throughput of the second transmit antenna is a little bit lower than that of the first transmit antenna.

One would expect from simulation results that Alamouti transmission greatly outperforms SISO transmission in such a strong frequency selective scenario (see Appendix A.2 for a simulation result in an ITU Pedestrian B channel). The gain of the Alamouti transmission over the SISO transmission is caused by the ability to "flatten" the frequency response of the channel by utilizing the spatial diversity. This, in turn, increases the probability of correctly decoding the received frame. Unfortunately, Alamouti transmissions are more sensitive to channel estimation errors than SISO transmissions (see, e.g., the derivation of the bit error probability of a 2×1 Alamouti transmission and a 1×2 transmission with maximum ratio combining in [26]). This results in a loss of all performance gains of the Alamouti coded system, as shown in Figure 5. In addition to the higher sensitivity of the Alamouti transmission to channel estimation errors, also the channel estimator performance in the Alamouti case is worse than in the SISO case. The reason for this lies in the fact that in a two-antenna transmission the available transmit power is split between antennas causing the received training to be of 3 dB lower SNR. In this scenario, the performance of the Alamouti transmission can be enhanced by a better channel estimator.

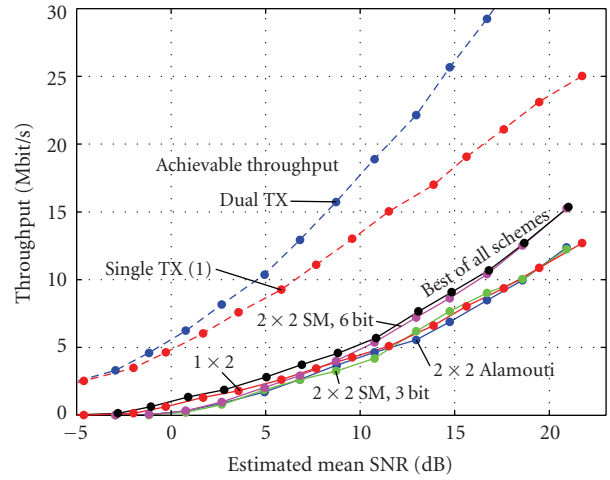

FIGURE 7: Scenario 1, measured (solid) and achievable (dashed) data throughput in the NLOS outdoor-to-indoor scenario using two receive antennas.

If, for example, LMMSE channel estimation is implemented, the Alamouti transmission could gain about 1.2 dB over the SISO transmission (see also Table 2 in Appendix B for a list of channel estimation gains).

The throughput results for the two-receive-antenna transmission in the same scenario are shown in Figure 6. Again, the Alamouti transmission performs worse than the single antenna transmission because of the same reasons described above. The spatial multiplexing scheme with 6-bit feedback allows for a throughput increase of about 20% at large transmit power. The spatial multiplexing scheme with only 3-bit feedback, that is, when only equal data rates are supported on both antennas, shows only the same performance as the Alamouti transmission. The curves show clearly that a throughput increase can only be achieved if the spatial coding is adapted on a per transmit antenna basis. In

our case, this is achieved by changing the coding rate, but the same effect may also be achieved by Alamouti coding with a subsequent power loading on the transmit antennas. This, however, requires that both power amplifiers are capable of transmitting at the full output power of the SISO system (3 dB more than in the MIMO case).

The "best of all schemes" curve shows the data throughput if the best transmission scheme is selected from the set of *all* possible AMC schemes at every receiver position (for every channel realization). This means that not only the AMC scheme is adapted to the channel but also the transmission mode, that is, single stream, Alamouti, or spatial multiplexing. In the low SNR region, the single stream transmission is selected most of the time; in the high SNR region, spatial multiplexing achieves the largest data throughput. Note that the "best of all schemes" throughput is sometimes larger than the throughput of the individual transmission modes. This is due to the individual selection of the transmission modes for every channel realization.

Figure 7 shows the throughput in the same scenario plotted over receive SNR. The throughput for the 1×2 system here is equal to the throughput of the 2×2 Alamouti system. In contrast, when these curves are plotted over transmit power, the 1×2 system shows an advantage of about 1 dB over the Alamouti system. When comparing systems with a different number of transmit antennas (e.g., SISO with Alamouti), we encounter the fact that the two transmit antennas do not have the same average channel gain. If those systems are compared over receive SNR, the throughput curves are shifted and, therefore, the results look different. For this reason, we plot all curves over transmit power rather than over receive SNR.

6.2. Scenario 2—NLOS outdoor-to-outdoor

In this scenario, the receive antennas were placed in a non-line-of-sight connection in the courtyard next to the building with the transmit antennas on the roof. The results for this scenario with strong frequency selectivity are shown in Figures 8 and 9. In contrast to the previous scenario, a transmission over the second transmit antenna leads to a *much* higher achievable throughput than a transmission over the first antenna. Therefore, adding the second antenna at the transmitter by Alamouti coding yields a significant throughput increase. On the other hand, if the SISO transmission had been performed over the second transmit antenna, Alamouti coding would have worsened the performance. We therefore conclude that in such a strongly asymmetric scenario, antenna selection is a promising alternative.

Figure 9 shows that the 2×2 transmission already achieves such a large SNR that the data throughput for the single stream transmission saturates (since no larger AMC values are available). In this SNR region, the usage of spatial multiplexing yields a large throughput increase. Also, due to the strongly asymmetric scenario, the 6-bit spatial multiplexing system greatly benefits from the adjustable code rate per transmit antenna.

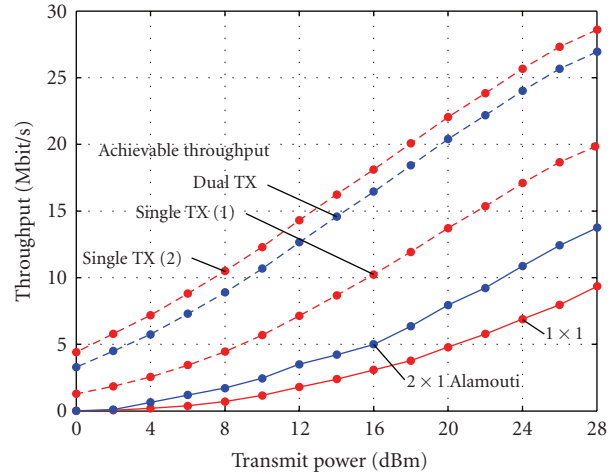

Figure 8: Scenario 2, measured (solid) and achievable (dashed) data throughput in the NLOS outdoor-to-outdoor scenario using one receive antenna. The largest transmit power corresponds to a receive SNR of about 24 dB.

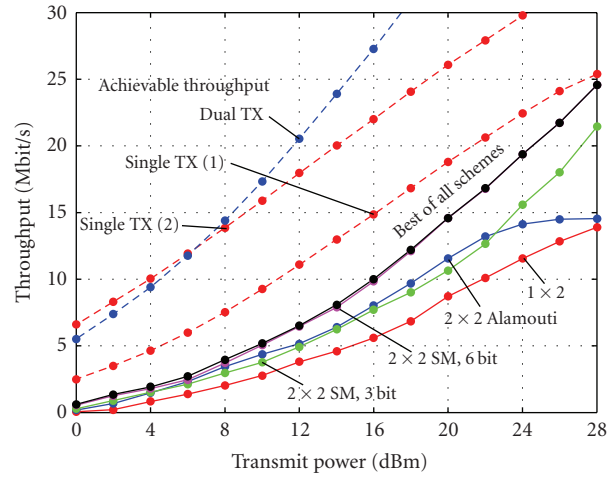

Figure 9: Scenario 2, measured (solid) and achievable (dashed) data throughput in the NLOS outdoor-to-outdoor scenario using two receive antennas. The largest transmit power corresponds to a receive SNR of about 24 dB.

6.3. Scenario 3—LOS outdoor-to-indoor

In this scenario, a line-of-sight connection was established by placing the receive antennas inside a building adjacent to the building with the transmit antennas on the roof. The measured data throughput is shown for one and two receive antennas in Figures 10 and 11, respectively. This scenario is characterized by a strong line-of-sight component leading to Rician distributed flat fading channels. The Rician K factor [27] was estimated to be $K = 2.9$. (The Rician K factor is defined as the relation between the energy of the nonfading line-of-site (specular) component and the energies of the diffuse fading components, $K = s^2/2\sigma^2$, given $\text{pdf}(x) = (x/\sigma^2)\exp-((x^2+s^2)/2\sigma^2)I_o(xs/2\sigma^2)$.)

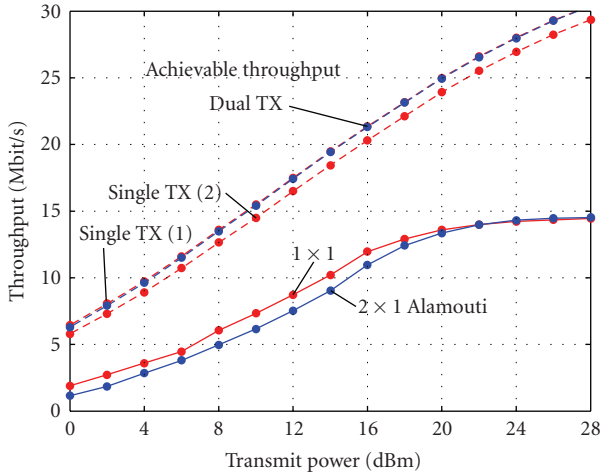

FIGURE 10: Scenario 3, measured (solid) and achievable (dashed) data throughput in the LOS outdoor-to-indoor scenario using one receive antenna. The largest transmit power corresponds to a receive SNR of about 32 dB.

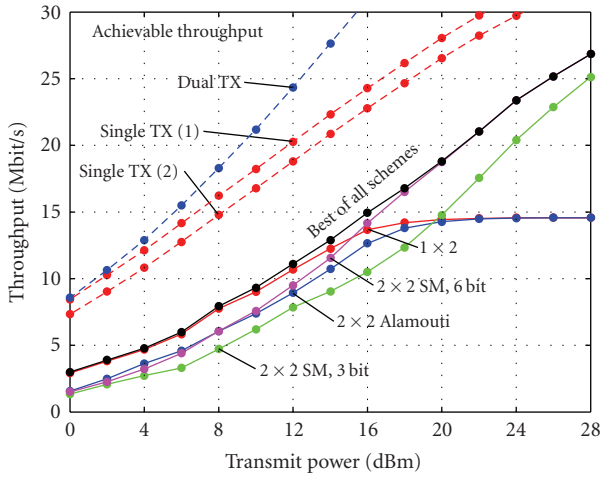

FIGURE 11: Scenario 3, measured (solid) and achievable (dashed) data throughput in the LOS outdoor-to-indoor scenario using two receive antennas. The largest transmit power corresponds to a receive SNR of about 32 dB.

The Alamouti code looses a lot of performance compared to the transmission with a single antenna. Here, in contrast to the previous two scenarios, the loss is caused by the flat fading channel (see Appendix A for simulation results). It is well known that in flat fading channels, the diversity can be increased by Alamouti coding. At a fixed modulation and coding scheme, the Alamouti coded system therefore has an increasing SNR advantage for large SNR values. However, since we are considering a coded system with adaptive modulation and coding, the operating points on the uncoded BER curves are between BER= 10^{-1} and BER= 10^{-2}. At these large BER values, the SNR gain due to Alamouti coding is only very small [28, pages 777–795] and vanishes when coded frame error rate or data throughput is plotted. Appendix A shows a simulation result for a flat fading Rice scenario (similar to the measured one) where the same effect can be observed. Additionally, Alamouti coding looses because of the poor channel estimation, as discussed above.

The 2×2 spatial multiplexing system suffers in this scenario from the line-of-sight component. For low transmit power, the performance is worse than the 1×2 performance. However, for large transmit power (>16 dBm), the throughput of the single stream transmission already saturates allowing for huge performance gains of the spatial multiplexing schemes. In such a scenario with a line-of-sight connection to the basestation, either new AMC values with larger data rate or spatial multiplexing should be implemented.

6.4. Discussion of the throughput loss

The measured throughput curves presented in the previous sections have in common that they are far (>10 dB) away from the achievable throughput. We identified the following factors as the main sources of the SNR loss.

(i) The largest loss is caused by the too simple convolutional channel coding which shows a relatively slow decline of the coded BER curve. The slow decline of the coded BER curve also leads to poor frame error ratio (FER) performance for large block lengths. (The frame error probability P_f for a frame of N_f bits can be calculated from the bit error probability P_b as $P_f = 1 - (1 - P_b)^{N_f}$.) As shown in Appendix A, the convolutional coding already costs >6.5 dB in SNR for a SISO transmission over a flat Rayleigh fading channel. Our preliminary assessments show that this loss can be decreased greatly if better channel codes (LDPC or Turbo codes) are employed.

(ii) According to the standard, only one OFDM training symbol per frame is used, leading to poor channel estimator performance. Additionally, in the MIMO transmissions, the power splitting between the two transmit antennas leads to the reception of the training with 3 dB smaller SNR, worsening the channel estimator performance. The implementation of a perfect (genie-driven) channel estimator that uses not only training but also the transmitted data symbols for channel estimation shows that a 2×1 Alamouti transmission can gain about 2.9 dB and a 1×1 SISO transmission can gain about 1.2 dB in SNR. If LMMSE channel estimation is employed, the 2×1 Alamouti system can gain about 1.8 dB and the 1×1 SISO system can gain about 0.6 dB over the corresponding systems with LS channel estimation. For a detailed list of values see Table 2 in Appendix B.

(iii) The set of possible combinations of modulations and code rates is suboptimal. The implemented feedback scheme can therefore be only optimal for this given set of AMC schemes.

7. CONCLUSIONS

In this paper, we investigated the throughput performance of SISO and MIMO WiMAX systems with limited feedback. Our evaluation is based on an extensive outdoor measurement campaign using practical setups of the basestation antennas and receiver positions. The comparison of the measured data throughput to the "achievable" data throughput, given by the mutual information of the channel, reveals a large loss (>10 dB in SNR). Even the single transmit antenna schemes only achieve a fraction of the possible data throughput. The largest part of this SNR/throughput loss is caused by the simple convolutional coding (about 6.5 dB). By using improved coding techniques (LDPC or Turbo codes), it should be possible to reduce this loss greatly. Another significant part of the SNR/throughput loss is caused by simple LS channel estimation. Depending on the transmission scheme, this loss is between 0.6 dB and 3.2 dB. The implementation of a WiMAX system therefore requires improved channel coding (e.g., the optional block Turbo code of the WiMAX standard) and enhanced channel estimators.

The comparisons between the different schemes revealed that Alamouti and spatial multiplexing transmissions (3-bit feedback) loose performance compared to SIMO and spatial multiplexing (6-bit feedback) transmissions. This is caused by the asymmetric gains of the MIMO channel. Therefore, also asymmetric transmission schemes are required to achieve high performance. Asymmetric transmission on two antennas can be accomplished by spatial multiplexing with individual coding and modulation for each transmit antenna, as investigated in the paper. Other possibilities may be, for example, transmit antenna selection or Alamouti transmission with subsequent power loading on the two transmit antennas. This, however, would require that both transmit amplifiers support the full transmit power of the SISO amplifiers (3 dB more than the MIMO amplifiers).

A very general conclusion of this work is that the overall performance of a communication system obviously depends on several factors. If a single part of a system is not implemented properly (e.g., channel coding, channel estimation), the overall system performance is substantially reduced. Only a thorough investigation comparing measured throughput to achievable throughput (given by the mutual information of the wireless channel) reveals whether all parts of a wireless system are properly configured. In the special case of WiMAX 802.16-2004, our performance analysis reveals that the optional channel coding schemes should be implemented before the optional MIMO extensions since advanced channel coding promises substantially larger gains.

APPENDICES

A. SIMULATIONS

In this appendix, we present some additional results confirming the statements in Section 6.

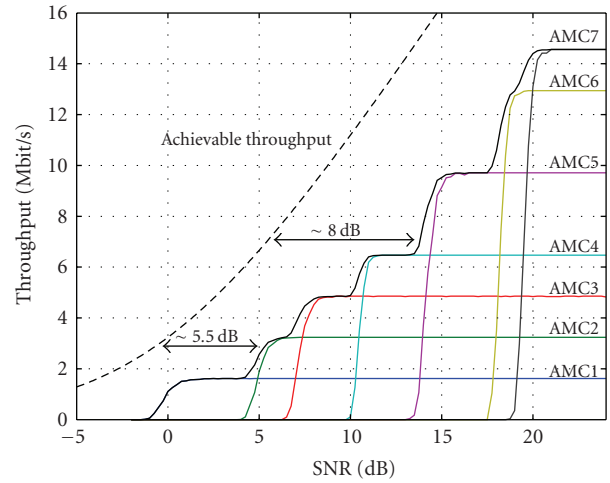

Figure 12: Simulated throughput performance of the SISO system with perfect channel knowledge in an AWGN channel.

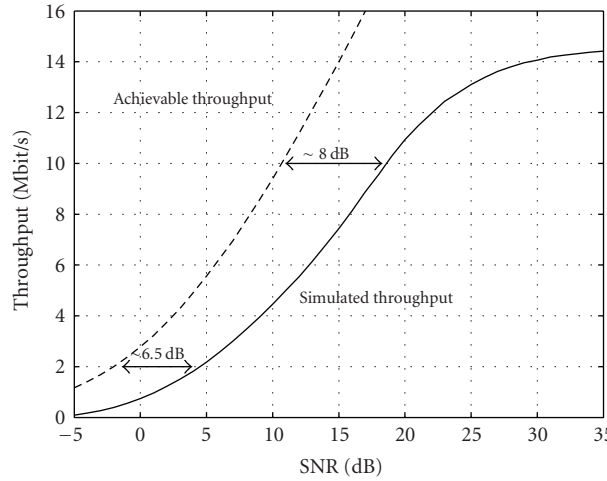

Figure 13: Simulated throughput performance of the SISO system with perfect channel knowledge in a flat Rayleigh fading channel.

A.1. SISO performance

In this section, we investigate the performance loss of the simple convolutional coding and the limited number of AMC schemes. As can be observed in the AWGN simulations in Figure 12, the loss to the achievable throughput is about 5.5 dB for AMC values one and two. For larger AMC values, where the convolutional coding is combined with puncturing to enable higher code rates, the corresponding loss is even higher. This is also reflected in Figure 13 where the throughput of a SISO system over a flat Rayleigh fading channel is plotted. The throughput loss here is about 6.5 dB for small SNR values and increases with the SNR. The reason for this increasing throughput loss is that at a specific (mean) SNR value the probability that the largest AMC value is selected increases. Since no larger AMC values are available, the throughput slowly saturates until it reaches its maximum.

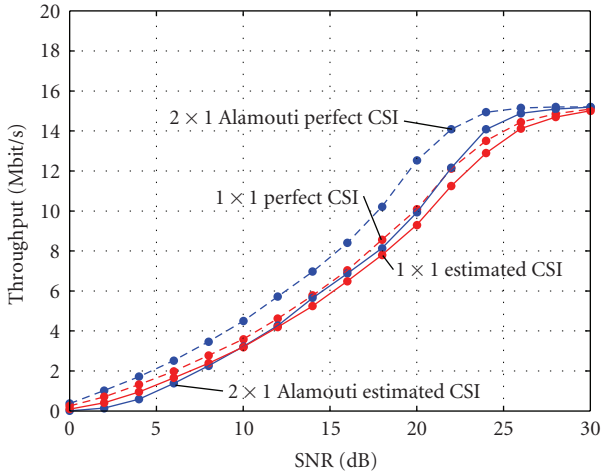

Figure 14: Simulated throughput performance for perfect and estimated channels, Pedestrian B channel model without spatial correlation.

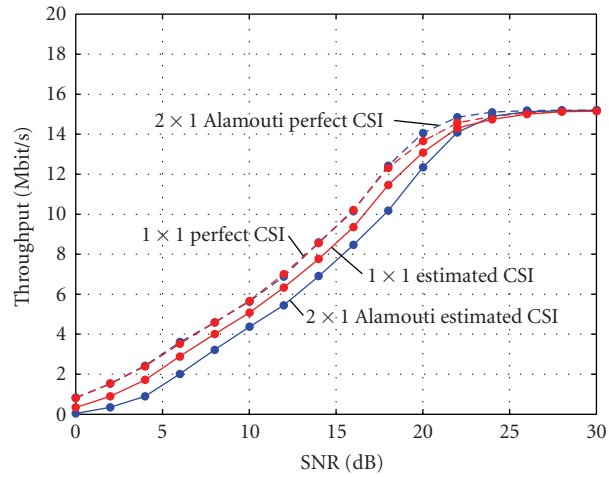

Figure 15: Simulated throughput performance for perfect and estimated channels, flat fading Rice channel with $K = 2.9$.

A.2. SNR loss due to channel estimation

A.2.1. Frequency selective channel

The first comparison (Figure 14) shows the simulated data throughput of the one receive antenna system in an ITU Pedestrian B [29] environment. No correlation was assumed between the transmit antennas. The figure shows the throughput for estimated and perfectly known channels. When perfect channel state information (CSI) is available at the receiver, the Alamouti transmission has superior performance over the SISO transmission throughout the entire SNR range. When the channel is estimated at the receiver, the Alamouti transmission looses about 2.4 dB in SNR, much more than the SISO (0.8 dB) leading to only slightly better performance of the Alamouti transmission in the high SNR region. One reason for the poor channel knowledge in the two-transmit-antenna case is the power splitting on the two transmit antennas. This leads to the reception of the training with 3 dB smaller SNR and, hence, a worse channel estimate than in the SISO case (see also Figure 4). Another reason for the poor channel estimate lies in the fact that the WiMAX standard defines only one OFDM training symbol per transmit antenna not allowing for an enhanced channel estimator that makes use of several training symbols.

A.2.2. Flat fading LOS scenario

In this simulation, we compare the throughput performance of 2×1 Alamouti transmission to the 1×1 SISO transmission in a flat fading Rice channel with $K = 2.9$. The results are plotted in Figure 15. When perfect channel state information is available at the receiver, the 2×1 and 1×1 systems show the same performance; only at a large SNR, Alamouti coded transmission has a small advantage. Since the system operates at a high uncoded BER, the diversity gain of the Alamouti code is not reflected in the data throughput. Note the difference to the previous simulation in the Pedestrian B environment where Alamouti has a 2 dB gain over the SISO transmission. In the frequency selective case, the Alamouti code "flattens" the frequency response and thus avoids deep fades (that would inhibit the correct decoding of the received frame) of some subcarriers. Therefore, space-time coding has the ability to increase the data throughput in frequency selective channels and not in flat fading channels.

Table 2: SNR gains of improved channel estimators over the LS estimator.

Scenario 1	LMMSE	genie-driven
1×1 SISO	0.6 dB	1.2 dB
2×1 Alamouti	1.8 dB	2.9 dB
1×2 SIMO	0.5 dB	1.2 dB
2×2 Alamouti	1.9 dB	3.2 dB
2×2 Spatial Multiplexing (3 bit)	1.4 dB	2.4 dB
2×2 Spatial Multiplexing (6 bit)	1.1 dB	2.2 dB

B. SNR GAINS OF IMPROVED CHANNEL ESTIMATORS

To quantify the SNR loss of the simple least-squares channel estimator, the received data were also evaluated with improved channel estimators. In particular, LMMSE channel estimation and genie-driven channel estimation were considered. The genie-driven estimator uses all transmitted data symbols (44 OFDM symbols) to obtain a channel estimate. Table 2 shows the SNR gains of these improved channel estimators over the least-squares estimator for measurement scenario one. In scenarios 2 and 3, the SNR gains of the improved channel estimators are approximately the same. A difference of only ±0.2 dB was observed [30].

ACKNOWLEDGMENTS

The authors would like to thank Arpad L. Scholtz, Lukas W. Mayer, Klaus Doppelhammer, Peter Brunmayr, Christian

Raschko, Robert Langwieser, Michael Fischer, and Werner Keim. Without their valuable contributions to the testbed, these measurements could not have been performed. The authors would also like to thank Professor Kathrein for providing the basestation antennas for their measurement campaign. This work has been funded by the Christian Doppler Laboratory for Design Methodology of Signal Processing Algorithms (see http://www.nt.tuwien.ac.at/cdlab/).

REFERENCES

[1] J. H. Winters, "On the capacity of radio communication systems with diversity in a rayleigh fading environment," *IEEE Journal on Selected Areas in Communications*, vol. 5, no. 5, pp. 871–878, 1987.

[2] G. J. Foschini and M. J. Gans, "On limits of wireless communication in a fading environment when using multiple antennas," *Wireless Personal Communications*, vol. 6, no. 3, pp. 311–335, 1998.

[3] E. Telatar, "Capacity of multi-antenna Gaussian channels," *European Transactions on Telecommunications*, vol. 10, no. 6, pp. 585–595, 1999.

[4] 3GPP, "Technical specification group radio access network; physical layer—general description," Tech. Rep. 25.201 V7.2.0, 3GPP, 2007, http://www.3gpp.org/ftp/Specs/archive/25_series/25.201/25201-720.zip.

[5] IEEE, "IEEE standard for local and metropolitan area networks; part 16: air interface for fixed broadband wireless access systems, IEEE Std. 802.16-2004," October 2004, http://standards.ieee.org/getieee802/download/802.16-2004.pdf.

[6] IEEE, "IEEE draft standard for local and metropolitan area networks; part 11: wireless LAN medium access control (MAC) and physical layer (PHY) specifications: amendment: enhancements for higher throughput, IEEE Draft Std. 802.11n(d2)," 2007.

[7] A. Hottinen, M. Kuusela, K. Hugl, J. Zhang, and B. Raghothaman, "Industrial embrace of smart antennas and MIMO," *IEEE Wireless Communications*, vol. 13, no. 4, pp. 8–16, 2006.

[8] P. Kyritsi, D. C. Cox, R. A. Valenzuela, and P. W. Wolniansky, "Capacity and rate performance of MIMO systems with channel state information at the transmitter," *IEEE Transactions on Wireless Communications*, vol. 5, no. 12, pp. 3469–3478, 2006.

[9] P. Xia, S. Zhou, and G. B. Giannakis, "Adaptive MIMO-OFDM based on partial channel state information," *IEEE Transactions on Signal Processing*, vol. 52, no. 1, pp. 202–213, 2004.

[10] J. C. Roh and B. D. Rao, "Multiple antenna channels with partial channel state information at the transmitter," *IEEE Transactions on Wireless Communications*, vol. 3, no. 2, pp. 677–688, 2004.

[11] http://www.nt.tuwien.ac.at/wimaxsimulator/.

[12] S. M. Alamouti, "A simple transmit diversity technique for wireless communications," *IEEE Journal on Selected Areas in Communications*, vol. 16, no. 8, pp. 1451–1458, 1998.

[13] A. Ghosh, D. R. Wolter, J. G. Andrews, and R. Chen, "Broadband wireless access with WiMax/802.16: current performance benchmarks, and future potential," *IEEE Communications Magazine*, vol. 43, no. 2, pp. 129–136, 2005.

[14] F. Wang, A. Ghosh, R. Love, et al., "IEEE 802.16e system performance: analysis and simulations," in *Proceedings of the 16th IEEE International Symposium on Personal, Indoor and Mobile Radio Communications (PIMRC '05)*, vol. 2, pp. 900–904, Berlin, Germany, September 2005.

[15] B. Muquet, E. Biglieri, and H. Sari, "MIMO link adaptation in mobile wimax systems," in *Proceedings of the IEEE Wireless Communications and Networking Conference (WCNC '07)*, pp. 1810–1813, Kowloon, Hong Kong, March 2007.

[16] T. H. Chan, M. Hamdi, C. Y. Cheung, and M. Ma, "Overview of rate adaptation algorithms based on MIMO technology in WiMAX networks," in *Proceedings of the IEEE Mobile WiMAX Symposium*, pp. 98–103, Orlando, Fla, USA, March 2007.

[17] A. F. Molisch, M. Steinbauer, M. Toeltsch, E. Bonek, and R. S. Thomä, "Capacity of MIMO systems based on measured wireless channels," *IEEE Journal on Selected Areas in Communications*, vol. 20, no. 3, pp. 561–569, 2002.

[18] R. E. Jaramillo, Ó. Fernández, and R. P. Torres, "Empirical analysis of a 2×2 MIMO channel in outdoor-indoor scenarios for BFWA applications," *IEEE Antennas and Propagation Magazine*, vol. 48, no. 6, pp. 57–69, 2006.

[19] D. Schafhuber, M. Rupp, G. Matz, and F. Hlawatsch, "Adaptive identification and tracking of doubly selective fading channels for wireless MIMO-OFDM systems," in *Proceedings of the 4th IEEE Workshop on Signal Processing Advances in Wireless Communications (SPAWC '03)*, pp. 417–421, Rome, Italy, June 2003.

[20] C. Studer, M. Wenk, A. P. Burg, and H. Bölcskei, "Soft-output sphere decoding: performance and implementation aspects," in *Proceedings of the 40th Asilomar Conference on Signals, Systems and Computers (ACSSC '06)*, pp. 2071–2076, Pacific Grove, Calif, USA, November 2006.

[21] M. Rupp, C. Mehlführer, S. Caban, R. Langwieser, L. W. Mayer, and A. L. Scholtz, "Testbeds and rapid prototyping in wireless system design," *EURASIP Newsletter*, vol. 17, no. 3, pp. 32–50, 2006.

[22] T. Kaiser, A. Wilzeck, M. Berentsen, and M. Rupp, "Prototyping for MIMO systems—an overview," in *Proceedings of the European Signal Processing Conference (EUSIPCO '04)*, pp. 681–688, Vienna, Austria, September 2004.

[23] S. Caban, C. Mehlführer, R. Langwieser, A. L. Scholtz, and M. Rupp, "Vienna MIMO testbed," *EURASIP Journal on Applied Signal Processing*, vol. 2006, Article ID 54868, 13 pages, 2006.

[24] Kathrein, "Technical specification Kathrein antenna type no. 742 211," http://www.kathrein.de/de/mca/produkte/download/9362108g.pdf.

[25] S. Caban and M. Rupp, "Impact of transmit antenna spacing on 2×1 Alamouti radio transmission," *Electronics Letters*, vol. 43, no. 4, pp. 198–199, 2007.

[26] D. Gu and C. Leung, "Performance analysis of transmit diversity scheme with imperfect channel estimation," *Electronics Letters*, vol. 39, no. 4, pp. 402–403, 2003.

[27] C. Tepedelenlioğlu, A. Abdi, and G. B. Giannakis, "The Ricean K factor: estimation and performance analysis," *IEEE Transactions on Wireless Communications*, vol. 2, no. 4, pp. 799–810, 2003.

[28] J. G. Proakis, Ed., *Digital Communications*, McGraw-Hill, New York, NY, USA, 3rd edition, 1995.

[29] "Recommendation ITU-R M.1225: Guidelines for evaluation of radio transmission technologies for IMT-2000," Tech. Rep., 1997.

[30] C. Mehlführer, S. Caban, and M. Rupp, "An accurate and low complex channel estimator for OFDM WiMAX," in *Proceedings of the 3rd International Symposium on Communications, Control, and Signal Processing (ISCCSP '08)*, pp. 922–926, St. Julians, Malta, March 2008.